Received 26 February 2024; revised 11 April 2024; accepted 5 May 2024. Date of publication 13 May 2024; date of current version 30 August 2024.

Digital Object Identifier 10.1109/OJCOMS.2024.3400273

Reconfigurable Intelligent Surface-Assisted Routing for Power-Constrained IoT Networks

RAWAN DERBAS[1], SHIMAA NASER[1] (Member, IEEE), LINA BARIAH[2] (Senior Member, IEEE), SAMI MUHAIDAT[1,3] (Senior Member, IEEE), LINA MOHJAZI[4] (Senior Member, IEEE), OSAMAH S. BADARNEH[5] (Senior Member, IEEE), AND ERNESTO DAMIANI[6,7] (Senior Member, IEEE)

[1]KU 6G Research Center, Department of Computer and Communication Engineering, Khalifa University, Abu Dhabi, UAE

[2]Technology Innovation Institute, Khalifa University, Abu Dhabi, UAE

[3]Department of Systems and Computer Engineering, Carleton University, Ottawa, ON K1S 5B6, Canada

[4]School of Engineering, University of Glasgow, G12 8QQ Glasgow, U.K.

[5]Electrical Engineering Department, School of Electrical Engineering and Information Technology, German Jordanian University, Amman 11180, Jordan

[6]Center for Cyber-Physical Systems, Department of Computer Science, Khalifa University, Abu Dhabi, UAE

[7]Secure Service-Oriented Architectures Research Laboratory, Milan, Italy

CORRESPONDING AUTHOR: S. NASER (e-mail: shimaa.naser@ku.ac.ae)

The work of Sami Muhaidat was supported in part by KU 6GRC under Project 84740005826G-RC.

ABSTRACT In power-constrained wireless networks, extending network lifespan can be achieved through effective energy harvesting techniques. Developing energy-efficient routing protocols in such networks is complex due to the unstable and unpredictable harvested energy. In this regard, reconfigurable Intelligent Surfaces (RIS), capable of manipulating the RF signals, offer enhanced energy harvesting, which in turn minimizes the nodes' battery recharging time (BRT). Our study presents a novel RIS-assisted routing protocol for multi-hop energy harvesting-based wireless networks. The protocol assigns channels to each hop on the chosen path. It incorporates a rate calculation algorithm that takes into consideration the harvested power, BRT, and channel conditions. More specifically, it assigns a specific rate to every available channel, taking into account the energy available at each node, the estimated time required for battery recharging, and the link status between nodes. By selecting the highest rate per hop, the protocol enhances network throughput while considering energy limits and channel quality. The proposed approach is evaluated and compared with the benchmark, the Min hop scheme, using MATLAB simulations, demonstrating its superior performance.

INDEX TERMS Battery recharging time, energy-efficient routing, IoT, reconfigurable intelligent surface (RIS), wireless power transfer (WPT).

I. INTRODUCTION

THE RISE of various wireless applications, driven by the proliferation of Internet-of-Things (IoT) technology, has spurred the evolution of wireless communication paradigms. This evolution aims to accommodate the projected network capacity and energy demands. Thus, IoT is envisioned to be the seed for the evolution of novel applications such as augmented reality (AR), autonomous driving, haptics, and e-health [1]. Nevertheless, with the anticipated exponential growth in the number of connected IoT devices in the coming years, upcoming wireless communication paradigms must accommodate dense network deployments while ensuring both low complexity and high energy efficiency [2]. It is worth noting that, due to the limited on-board capabilities of IoT devices, multi-hop communication is necessary to meet certain quality of Service (QoS) requirements. In addition to expanding the network coverage and reducing the transmission power consumption, multi-hop networks have the potential to increase the overall network throughput by using multiple nodes as relays instead of a long single-hop. However, depending solely on the batteries of the devices

in multi-hop communications could result in communication disruptions and delays in packet transmission. Furthermore, in extreme and inaccessible conditions, such IoT devices require frequent batteries replacement and recharging plugins, which is cost-inefficient, difficult, and hazardous. This has motivated significant endeavors aimed at developing energy-efficient strategies to prolong the lifespan of these networks [3].

Motivated by the technological advancements in the field of Radio Frequency Energy Harvesting (RFEH), a wide range of ambient energy sources can be scavenged and converted into electrical energy to power the circuits of IoT devices. These energy sources include electromagnetic radiation (EM) from WLAN access points, cellular base stations, TV broadcasting stations, and AM/FM radio stations, to name a few. This technique paved the way for developing batteryless systems, addressing the environmental impacts of battery manufacturing and disposal. Besides that, in large-scale IoT networks, the costs of recharging a substantial number of batteries are significantly high [4]. Despite the benefits mentioned above, RFEH still faces some challenges, such as the high unpredictability, limited availability, and uncontrollable nature of ambient EM radiation. Thus, only a portion of the energy emitted by an energy transmitter can be harvested by an energy receiver (ER). This limitation necessitates efficient circuit design to enhance RF-to-DC conversion efficiency while ensuring a small size for the harvester [5].

To overcome the limitations of ambient RFEH and ensure continuous energy replenishment for resource-constrained devices, wireless power transmission (WPT) has been proposed as a prominent paradigm to power those devices through a dedicated and fully controlled RF power source. Thus, instead of passively harvesting ambient energy, resource-constrained devices can harvest power from dedicated RF signals to charge their batteries [6]. Nevertheless, the random nature of the wireless environment is still challenging, as it can lead to random and unpredictable variations in signal strength, interference, and fading, which affects the efficiency of power transfer, limiting the power harvesting capabilities. Recently, researchers have directed their attention toward advancing technologies like massive multiple-input multiple-output (MIMO) and relays to boost the efficiency of WPT-enabled systems. Nonetheless, implementing these technologies poses certain limitations, including increased energy consumption, computational complexity, and hardware costs, which become more pronounced when dealing with higher frequencies, such as millimeter-wave. Furthermore, the efficiency of WPT using these conventional technologies is not only limited by the distance between the energy transmitter and the ER but also by the RF signal attenuation due to various impairments. These include deep multipath fading, severe attenuation, blockage, and Doppler shift [7].

Reconfigurable intelligent surfaces (RISs) have recently attracted widespread interest within the wireless research community due to the unique prospect of controlling the unpredictable propagation of radio waves in wireless channels [8]. This technology has enabled an entirely new concept, where the RF signal characteristics can be tuned to enable reconfigurable control over the wireless environment. RIS structures comprise electronically configurable reflective elements (REs) that can manipulate the phase of incoming signals. Consequently, RISs can yield various advantageous effects, such as establishing artificial line-of-sight links, introducing additional propagation paths, and enhancing the statistical characteristics of the channel between the transmitter and receiver [9]. Such functionalities enable the RISs to direct RF signals towards a particular node in the network. These advantages paved the way for the RISs to be utilized in many applications, such as WPT-enabled IoT networks. Taking advantage of intelligent EM signal control, particularly in regions lacking coverage, the utilization of RISs increases the harvested energy and improves the network's overall performance.

As energy harvesting gains increase significantly, it becomes crucial to develop algorithms that efficiently harness this harvested power. These algorithms play a significant role in maximizing the benefits of energy harvesting and ensuring its effective utilization to power network devices, which is further underscored when attempting to network with a large number of low-power devices. In the context of multi-hop communications, energy-aware routing algorithms need to be designed to consider energy consumption in several ways. For example, prioritizing paths that require lower energy by considering the energy levels at the nodes, thereby minimizing the risk of power depletion. Moreover, these algorithms can distribute and balance the energy load evenly among the network nodes, preventing some nodes from depleting rapidly while others have excess energy. A key metric that determines the performance of the harvested energy, and thus can be adopted to design efficient EH algorithms, is the time that it takes to recharge the batteries of the IoT devices, known as battery recharging time (BRT). BRT depends on multiple factors, such as the efficiency of the energy conversion process, battery characteristics, and, most importantly, the RF propagation environment. Because of the unpredictable nature of the wireless propagation environment, the energy harvesting process is subject to randomness, making the amount of harvested energy depend on time and battery conditions. Hence, it is essential to develop statistical models that effectively capture and describe the impact of system parameters on the energy harvesting process. These models are necessary for quantifying the accumulated energy over time and enabling the selection of proper battery-related performance parameters, such as capacity and discharging depth. Additionally, they facilitate in determining the state-of-charge, which plays a vital role in storing the harvested energy [10].

Motivated by the above, and by leveraging the merits of the RISs to enhance the efficiency of WPT-assisted systems and improve the BRT, in this work, we aim to develop an energy-aware (EA) routing for IoT networks, exploiting

the energy harvesting to support multi-hop communication. In particular, we propose an optimized route selection technique that relies on selecting the route that maximizes the throughput by considering the joint relationship between the channel conditions and the amount of the harvested energy (in terms of BRT).

A. RELATED WORK

The exponential growth of IoT devices has necessitated the development of energy-efficient routing protocols to extend network lifetimes. For instance, a novel joint multi-hop EA routing protocol was proposed in [11] to enhance the overall network lifetime. Furthermore, the authors in [12] presented a joint EA and secure routing protocol in multi-hop networks. A clustering-based routing protocol designed for effective implementation in multi-hop large-scale IoT networks was proposed in [13]. This protocol relies on occasionally changing the clusterhead to balance the power consumption among nodes in the same cluster. The authors of [14] proposed an energy harvesting routing (EHR) protocol to improve energy utilization by prioritizing energy harvesting. The EHR protocol comprises two key phases: a hybrid routing metric combining energy harvesting and residual energy parameters; and an updating algorithm allowing each node to maintain the dynamic energy information of its neighbors. By jointly utilizing this information and the hybrid metric, the EHR protocol efficiently selects the best next hop for data transmission. On the other hand, the authors in [15] introduced an Energy-opportunistic Weighted Minimum Energy (E-WME) algorithm for a wireless sensors network. The cost of each node is computed by considering both the available energy and energy harvesting rate.

Although the routing frameworks in [11], [12], [13], [14], [15] effectively reduce energy consumption and extend the nodes' lifespan, they come with inherent limitations. For example, these protocols passively harvest RF energy from the environment and do not consider the actual amount of energy accumulated over the harvesting period. Moreover, these works assumed a constant replenishment rate for all nodes, which makes them unsuitable to deal with the stochastic characteristics of the ambient energy sources. Motivated by the significant benefits of WPT to wirelessly charge devices' batteries through a dedicated and fully controlled RF power source, the authors of [16] studied the use of WPT technology in low-power and lossy network (RPL) model, where they proposed a new objective function for RPL, which jointly considers the energy consumption of intermediate nodes and the amount of recharging energy available from the received power of a child node. Simulation results demonstrated that the proposed algorithm efficiently minimizes the energy loss and extends the network lifetime by selecting the most efficient path via the sink. However, the efficiency of such algorithms is limited by the distance between the transmitter and receiver.

Because of their large aperture, RISs are leveraged to power a massive number of devices, compensating for the significant power loss over long distances [17], [18], [19]. For instance, by adjusting the phase and amplitude of the incident waves, RISs can focus the energy toward the intended node, thus reducing losses and improving overall transfer efficiency. Furthermore, RIS can extend the WPT range by actively controlling electromagnetic wave propagation. Finally, RISs can dynamically adapt to changes in the environment or the positions of the node, which allows better optimization of the power transfer in real-time, taking into consideration the variations in signal strength, interference, and other environmental factors. Motivated by these capabilities of RISs, different works in the literature have considered the integration of RISs for dynamic resource allocation and routing protocols. In particular, the authors of [17] considered installing the RIS on an aerial platform to exploit rich LoS communications for an energy-efficient aerial backhaul system. Similarly, the authors in [18] considered the RIS-aided Unmanned Aerial Vehicles (UAVs)-enabled integrated access and backhaul (IAB) network targeting energy-efficient operations. They proposed a dynamic resource management framework that optimizes the end-to-end power consumption and data rate by adjusting controllable parameters such as RIS phase shifts, bandwidth split, and transmission powers of users and UAVs. Furthermore, a mobile ad-hoc RIS-assisted routing scheme was investigated in [19]. Specifically, the RIS was considered to support the data flow in multipath routing, minimize the delay in the path discovery phase, and avoid co-channel interference, leading to lower overall energy consumption in the network. Furthermore, gaining insight into the statistical characteristics of the amount of collected energy, which is proportional to the received RF signal strength, can also enable an efficient optimization of available energy resources. These characteristics facilitate the development of energy management algorithms and protocols that can intelligently allocate energy based on its statistical characteristics. Also, studying the dynamic nature of the ambient resources can help the development of adaptive algorithms that can handle the fluctuations in energy availability and extend the system's operational lifetime, improving the overall system performance.

As previously stated, BRT is considered an important performance metric for RFEH systems, which is also considered a random process due to its dependence on the RF propagation environment. Few studies are carried out to develop statistical models of the BRT for traditional WPT systems operating over different multipath fading channels [20], [21]. Their findings revealed that the RFEH process depends on various factors such as channel fading, system, and battery parameters, i.e., discharge depth, capacity, and BRT, to name a few. To boost the amount of the harvested energy, the authors of [22] developed a single-user BRT statistical framework for RIS-assisted WPT systems by considering Rayleigh fading channels. They presented a statistical analysis of the proposed system, including the probability density function (PDF) and cumulative

distribution function (CDF) of the instantaneous received power. Based on this, approximate closed-form expressions for the PDF, CDF, and moments of the BRT are derived as functions of the received power, battery parameters, and the number of RIS REs. In [23], the authors designed a routing algorithm that considers the BRT as a metric to study the performance of multi-hop IoT networks in terms of throughput. However, the energy harvesting capability can be further improved by utilizing RIS, thanks to their ability to manipulate and redirect RF signals towards specific nodes, thereby enhancing the amount of the harvested energy and minimizing the nodes' BRT. Based on the conducted literature review, it becomes obvious that no prior studies have explored the benefits of employing RIS to improve the energy harvesting capabilities of the nodes, hence reducing the BRT, which is used as a key parameter in our proposed routing protocol. In particular, we propose an optimized route selection technique that relies on selecting the route that maximizes the throughput by considering the joint relationship between the channel conditions and nodes' BRT. In this work, we adopt the framework presented in [22] as a foundation to develop a new statistical model based on the double Beaulieu–Xie (BX) fading channel [24]. Nonetheless, it is worth noting that the authors in [22] did not study the effect of the direct link blockage. Therefore, in this work, we develop a framework that takes into consideration the presence of random blockage in the direct link. The proposed framework will be then leveraged to develop a RIS-assisted EA routing protocol tailored for energy-constrained devices equipped with energy harvesting capability. The protocol aims to optimize the channel assignment and route selection mechanisms, ensuring that the intermediate links in the routing process achieve the highest rates for the intended source-destination (SD) pair. The proposed scheme is compared with the minimum hop (Min Hop) scheme as a benchmark. The minimum hop algorithm, also known as the shortest path algorithm, is a routing technique employed to discover the path that involves the least number of hops between two nodes within a network [25]. Our proposed algorithm aims to optimize the network performance by choosing the path that offers the best possible data rate among different paths, determined by the weakest (minimum rate) link in each path. The goal of this is to ensure a more balanced and efficient network usage, as it promotes equitable resource distribution. On the contrary, the Min hop algorithm mainly focuses on the shortest distance or least number of hops regardless of the bandwidth or the quality of the path. By considering the overall quality and capacity of the entire path, the proposed algorithm leads to a potentially higher network throughput and improved reliability in diverse network conditions.

B. MOTIVATION AND CONTRIBUTION

In this work, we propose a routing scheme that leverages RIS technology to improve the efficiency of energy usage in node batteries, thereby enhancing their recharging time. By utilizing an ambient RF source and designing a two-phase harvest-then-transmit scheme, our protocol aims to maximize the utilization of harvested power for data transmission. The protocol combines the harvested energy from both the RIS and direct links during the harvest phase. Subsequently, it utilizes the harvested power during the transmit phase to optimize energy efficiency. In order to investigate the underlying system model under a practical channel model, we consider the BX fading channel, which models the presence of LoS component. The BX fading model has gained considerable attention in theoretical research and experimental measurement data validation. Derived from the normalization of the non-central chi-distribution, similarly, in the way that the Nakagami-m distribution was obtained from the central chi-distribution, this model adheres to the physical requirement of power conservation, and it is particularly well-suited for characterizing wireless channels that exhibit multiple LoS and non-LoS components [26], [27]. With its flexibility, the BX fading model is characterized by way of its parameter m that unifies the Rayleigh, Ricean, $\kappa - \mu$, and Nakagami-m fading models. To elaborate further, the Nakagami-m model is regarded as a specific case of the BX fading model in the absence of the Line of Sight (LOS) component. This is analogous to the Rayleigh fading model, which serves as a special case of the Ricean fading model in the absence of the LOS component. Furthermore, the BX fading model transforms into the Ricean fading model when the value of m is set to one, much like how the Nakagami-m model turns into the Rayleigh fading model under the same value of m [28], [29]. To the best of our knowledge, this is the first routing protocol to exploit RIS for battery recharging in IoT devices. The main contributions of this work can be summarized as follows:

- A tight approximation for the PDF and the CDF of the instantaneous received power between the BS and the ER node are obtained under the assumption of BX distributed channel models and the presence of a random blockage in the direct link. Such approximation enables the accurate modeling and analysis of the amount of the harvested energy, which directly impacts the proposed protocol's performance.
- Capitalizing on the derived expressions, closed-form expressions for the PDF and CDF of the BRT are obtained. These statistical measures provide valuable insights into the duration necessary for battery recharging, directly affecting the amount of power available for data transmission. Extensive results are presented to accurately depict the effect of the battery parameters on the network performance.
- The energy consumption and latency of the IoT network are optimized by designing a routing protocol that relies on selecting optimum routes by quantifying the battery recharging time. Therefore, a RIS-assisted energy-aware routing protocol, namely RIS-assisted EAR, is designed for wireless networks. Using an RIS, the RF signal is manipulated and redirected towards the nodes,

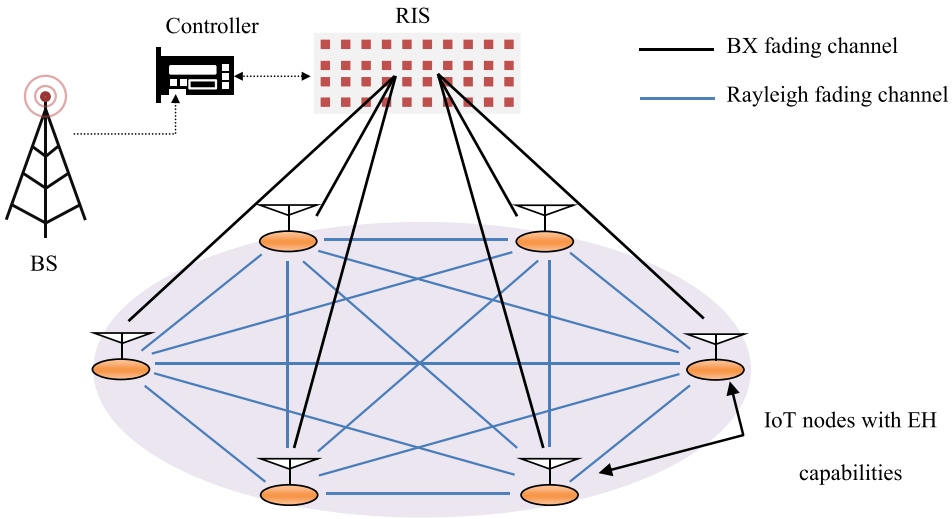

FIGURE 1. Proposed system model within $A \times A$ m^2 area.

facilitating the battery recharging of the IoT nodes. Moreover, the proposed protocol can make decisions by considering the available energy and optimizing the selection of channels and paths to achieve the highest achievable data transmission rate.

- The performance of the developed routing protocol is evaluated through conducting extensive simulation, taking into account a variety of network parameters, including the number of REs, transmitted power, battery capacity, and the number of available channels.

C. ORGANIZATION

The remainder of this article is arranged as follows: in Section II, the RIS-assisted routing protocol system model is presented, and the BRT statistical analysis expression of the RIS-assisted WPT system is presented. Section III describes RIS-assisted EAR problem statement and formulation. This section also introduces the solution of the RIS-assisted EAR problem. A performance evaluation is discussed in Section IV. Finally, Section V provides some concluding remarks and future research possibilities.

Notations: The functions $F_X(.)$ and $f_X(.)$ represent the random variable's cumulative distribution function (CDF) and probability density function (PDF), respectively. Moreover, $|.|$ and $\mathbb{E}(.)$ denote the absolute value and expectation operator, respectively. Finally, $\Gamma(.)$, $L_a^q(.)$, and $G_{p,q}^{m,n}(.|.)$ denote the complete Gamma functions, the q-th order Laguerre polynomial, and the Meijer G-function, respectively.

II. NETWORK AND CHANNEL MODEL

A. NETWORK SETTING

This work considers a wireless network with N_u nodes, placed randomly within an area of size A $\times$ A m^2, and a base station (BS). Also, a single RIS with M REs is considered to assist with the WPT between the BS and the N_u nodes, as illustrated in Fig. 1. The direct link between the BS and the node is assumed to experience strong line-of-sight, i.e., no fading, with a random blockage probability.

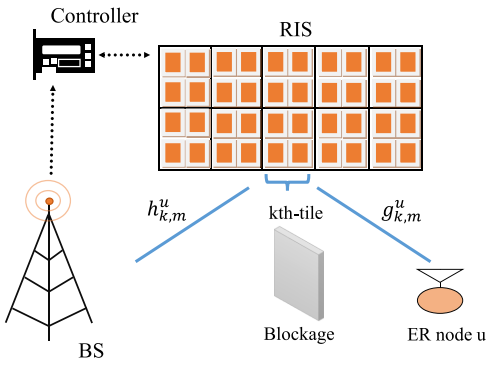

FIGURE 2. E2E single node channel gain.

The RIS is partitioned into K tiles with $G = \frac{M}{K}$ elements. Each tile is associated with a single node, denoted as K_u, as shown in Fig. 2. It is noteworthy that the number of associated tiles, denoted as $\hat{K}$, depends on the number of the nodes that have harvested power falls below a specified threshold $P_{h_{\text{th}}}$. In other words, the maximum number of nodes that can be harvested simultaneously is limited by K, thereby ensuring that $\hat{K} \leq K$. It is also assumed that each node has only one antenna (i.e., nodes either harvest energy or transmit data at a particular time slot). The nodes adopt a time-switching policy that divides the frame into two portions to perform the EH and the information transmission functionalities [30]. Specifically, the time portion ν_u is used for EH, and the remaining $1 - \nu_u$ is used for information transmission, where $0 \leq \nu_u \leq 1$. For simplicity, we assume ν_u is fixed and the same for all nodes. It is important to highlight that optimizing this ratio, ν_u, is crucial for different reasons and can be considered in future work. First, optimizing ν_u ensures that nodes have sufficient energy storage for the next data transmission phase. This maintains uninterrupted data transmission and processing, which ultimately leads to improved network performance and data delivery. Also, given that energy availability can

TABLE 1. Mathematical operators and functions definitions.

Notation	Explanation	Notation	Explanation
$A \times A$	Area (m^2)	N_u	IoT ER nodes
M	Number of RIS elements	K	Number of RIS tiles
G	Number of elements in each tile	ν_u	The time portion for energy harvesting
ξ	Probability of blockage	$h^u_{k,m}$, and $g^u_{k,m}$	The channel coefficients between the BS-RIS and RIS-u, respectively.
$Y^u_{k,m}$	The coefficient of the mth RE in the kth tile	λ, Ω, and m	The scale parameters of BX fading channels
$\theta^u_{k,m}$, and $\psi^u_{k,m}$	The channel phase between the BS-RIS and RIS-u, respectively.	P_t^{BS}	The BS transmitted power
$d_1, d_{2,u}$ and $d_{3,u}$	The distances of BS-RIS, RIS-u, and BS-u, respectively.	P^u_r	The received power at node u in the energy harvesting phase
T^u_r	The instantaneous BRT of node u	P^u_h	The harvested power at node u
α	The conversion coefficient	V_b	The constant battery operating voltage
D_d	The discharge depth	C_b	The battery capacity
η	RF-to-DC signal conversation factor	δ	The pathloss exponent
Q_u	E2E channel gain from the BS to node u	$\hat{h}$	Denotes for hops
$\hat{w}$	Denotes for routes	$\mathcal{C}$	The set of channels
SNR	signal-to-noise ratio	$\text{SNR}^{(c)}_{\hat{w},\hat{h}}$	The SNR for each channel c over each hop $\hat{h}$ in each route $\hat{w}$
γ^*	SNR threshold	$\mathcal{C}^*_{\hat{w},\hat{h}}$	The set of available channel with SNR greater than γ^*
$P_{h_{\text{th}}}$	The minimum harvested power	${N_u}^*$	The nodes that have harvested power greater than $P_{h_{\text{th}}}$
τ^*_r	BRT threshold	BW	The available channels bandwidth
$P^{(c)}_o$	The pathloss over channel c	G_t and G_r	The gain of the transmit antenna and the gain of the receive antenna
$B^{(c)}_{\hat{h},\hat{w}}$	the channel fading coefficient between any ER pair	$d^{(c)}_o$	The reference distance
$\lambda^{(c)}$	The operating wavelength	d	the distance between any two communicating nodes
$P^{(c)}_{r_{\hat{h},\hat{w}}}$	The received power at node $u+1$ over each channel c over each hop $\hat{h}$ in each route $\hat{w}$	$R^{(c)}_{\hat{w},\hat{h}}$	The achieved transmission rate at node $u+1$ over each channel c over each hop $\hat{h}$ in each route $\hat{w}$
$U_S - U_D$	Source-destination pair	$\mathcal{W}$	the number of possible routes
$\mathcal{H}$	the number of hops in each route	$\hat{w}^*$	The chosen route
$\mathcal{N}_o$	the power spectral density (PSD) of the thermal noise	$\mathcal{Z}^{(c)}_{\hat{w},\hat{h}}$	1, if channel c is assigned to hop $\hat{h}$ along route

vary over time and across different locations within the network, optimizing the time-switching ratio allows nodes to adapt dynamically to these changes, ensuring optimal energy utilization regardless of environmental changes. For convenience, we define an indicator function to denote the mode switching of node u as follows

$$\rho_u = \begin{cases} 1, & \text{Transmission mode is active} \\ 0, & \text{EH mode is active} \end{cases} \quad (1)$$

B. CHANNEL MODEL BETWEEN THE BS AND AN ER NODE

In order to consider a practical channel model, the BX fading model [31] is adopted here to characterize the received signal at each ER node. The BX model incorporates both the diffuse scatter component and the LoS component. As shown in Fig. 2, the direct link between the BS and node u is assumed to experience strong line-of-sight, with a random blockage probability ξ. The presence of the blockage is characterized as a Bernoulli random variable J, where $J \in [0, 1]$. We denote by $h^u_{k,m} \triangleq |h^u_{k,m}|e^{j\theta^u_{k,m}}$ the equivalent fading channel between the BS and the mth element in the kth tile of the RIS, where $m \in [1, 2, \ldots, G]$, and $k \in [1, 2, \ldots, K]$, and by $g^u_{k,m} \triangleq |g^u_{k,m}|e^{j\psi^u_{k,m}}$ the fading channel between the mth element in the kth tile of the RIS and the node u. Also, the magnitudes of $h^u_{k,m}$ and $g^u_{k,m}$ (i.e., $|h^u_{k,m}|$ and $|g^u_{k,m}|$) are considered as independent and identically distributed (i.i.d) BX fading channels with scale parameters Ω_1, λ_1, m_1, for $h^u_{k,m}$ and Ω_2, λ_2, and m_2 for $g^u_{k,m}$, where k and m refers to the mth element in the kth of the RIS. For simplicity, the scale parameters are assumed to be the same for both links (i.e., $\Omega_1 = \Omega_2 =$, $\lambda_1 = \lambda_2$, and $m_1 = m_2$). Additionally, the phases $\theta^u_{k,m}$ and $\psi^u_{k,m}$ are uniformly distributed in $[-\pi, \pi]$.

The RIS reflects the signal transmitted from the BS to the nodes, which is subsequently harvested and stored in finite-capacity batteries for future packet transmissions. The instantaneous received power at node u can be expressed as

$$P_r^u = \nu_u \left(\frac{\left| \sum_{m=1}^{G} h_{k,m}^u y_{k,m}^u g_{k,m}^u \right|^2}{\left(d_1 d_{2,u}\right)^\delta} P_t^{BS} + \frac{P_t^{BS}}{\left(d_{3,u}\right)^\delta} J \right), \quad (2)$$

where P_t^{BS}, δ, d_1, $d_{2,u}$ and $d_{3,u}$ refer to the transmitted power from the BS, the pathloss exponent, the distance between BS and the *kth* tile, the distance between *kth* tile and node u, and the distance between the BS and node u, respectively. Assuming that the channel phases are perfectly known (i.e., $\theta_{k,m}^u$ and $\psi_{k,m}^u$), and without loss of generality, the coefficient of the *mth* RE in the *kth* tile can be expressed as [32]

$$y_{k,m}^u = |y_{k,m}^u| e^{-j\Phi_{k,m}^u} \quad (3)$$

where $|y_{k,m}^u| \in [0, 1]$ and $\Phi_{k,m}^u \in [-\pi, \pi]$ are the reflection amplitude and the phase shift of the *mth* RE in the *kth* tile. It is worth noting that $\Phi_{k,m}^u$ is chosen to compensate for the phase shift of the cascaded channels, i.e., $\Phi_{k,m}^u = -(\theta_{k,m}^u + \psi_{k,m}^u)$, to maximize the instantaneous signal-to-ratio (SNR). Also, we assume that $y_{k,m}^u$ is normalized to unity [33]. Accordingly, (2) can be rewritten as

$$P_r^u = \nu_u \left(\frac{P_t^{BS}}{\left(d_1 d_{2,u}\right)^\delta} Q_u^2 + \frac{P_t^{BS}}{\left(d_{3,u}\right)^\delta} J \right), \quad (4)$$

where

$$Q_u = \sum_{m=1}^{G} |h_{k,m}^u| |g_{k,m}^u| \quad (5)$$

is the end-to-end (E2E) channel gain of the node u. It can be readily observed from (5) that the effects of the channel of the RF source on the received power (and accordingly on the battery recharging time) can be statistically defined.

1) THE *n*TH MOMENT OF DOUBLE BX RANDOM VARIABLE

Noting that Q_u represents a sum of the product of two independent BX random variables (RVs), the nth moment of a BX distributed RV is given in [31, Eq. (9)], as

$$\mu(n) = \left(\frac{m_1}{\Omega_1}\right)^{-\frac{n}{2}} \Gamma\left(1 + \frac{n}{2}\right) L_{\frac{n}{2}}^{(m_1-1)}\left(-\frac{m_1}{\Omega_1}\lambda_1^2\right) \quad (6)$$

where $\Gamma(.)$ and L_a^q are the complete Gamma function [34] and the q-th order Laguerre polynomial [35], respectively. Hence, the nth moment of the double BX fading model can be evaluated by the product of the individual moments as in (7) on the bottom of the next page.

2) THE PDF OF Q_u

The PDF of Q_u can be written in an accurate closed-form approximation using the moment-based density approximation scheme proposed in [36] as

$$f_{Q_u}(x) = a_1 G_{1,2}^{2,0}\left(\frac{x}{a_2}\middle| \begin{matrix} -; a_3 \\ a_4, a_5; - \end{matrix}\right), x \geq 0 \quad (8)$$

where $G_{\cdots}^{\cdots}(.|.)$ is the standard Meijer G-function and the parameters a_1, a_2, a_3, a_4, and a_5 are calculated based on n [36, Eq. (3) - Eq. (10)]. It is worth mentioning that the moments of Q_u can be obtained by first deriving the first four moments of the double BX model, then employing the multinomial theorem to find the first four moments of Q_u [37, Eq. (53) - Eq. (56)]. Based on the derived PDF in (8), an accurate approximation of the CDF of Q_u can be analytically computed as follows [36]

$$F_{Q_u}(x) = a_1 a_2 G_{2,3}^{2,1}\left(\frac{x}{a_2}\middle| \begin{matrix} 1, a_3 + 1 \\ a_4 + 1, a_5 + 1; 0 \end{matrix}\right), x \geq 0 \quad (9)$$

3) STATISTICAL CHARACTERIZATION OF THE RECEIVED POWER

Since J follows a Bernoulli distribution with probability $p(J = 1) = \xi$ and probability $p(J = 0) = 1-\xi$, the PDF of P_r^u can be found by applying the transformation of random variables using (4) as follows

$$f_{P_r^u}(x) = (1 - \xi) f_{P_r^u}(x|J = 0) + \xi f_{P_r^u}(x|J = 1), \quad (10)$$

When $J = 0$, (4) can be rewritten as $P_r^u = k_1 Q_u^2$, where $k_1 = \frac{\nu_u P_t^{BS}}{(d_1 d_{2,u})^\delta}$. While, in case $J = 1$, (4) can be rewritten as $P_r^u = k_1 Q_u^2 + k_2$, where $k_2 = \frac{\nu_u P_t^{BS}}{(d_{3,u})^\delta}$. By applying these random variables transformations, the PDF of the received power at node u can be written as in (11) on the bottom of the page.

Taking into account (4), it is straightforward to note that the relation between the CDFs of the E2E channel gain Q_u and the received power can be given as

$$F_{P_r^u}(x) = Pr\left(P_r^u \leq x\right) \quad (12)$$

$$\mu(n) = \left(\frac{m_1 m_2}{\Omega_1 \Omega_2}\right)^{-\frac{n}{2}} \left(\Gamma\left(1 + \frac{n}{2}\right)\right)^2 L_{\frac{n}{2}}^{(m_1-1)}\left(-\frac{m_1}{\Omega_1}\lambda_1^2\right) L_{\frac{n}{2}}^{(m_2-1)}\left(-\frac{m_2}{\Omega_2}\lambda_2^2\right). \quad (7)$$

$$f_{P_r^u}(x) = (1 - \xi)\frac{a_1 a_2}{2x} G_{1,2}^{2,0}\left(\frac{\sqrt{\frac{x}{k_1}}}{a_2}\middle| \begin{matrix} -; a_3 + 1 \\ a_4 + 1, a_5 + 1; - \end{matrix}\right) + \frac{\xi a_1 a_2}{2(x - k_2)} G_{1,2}^{2,0}\left(\frac{\sqrt{\frac{(x-k_2)}{k_1}}}{a_2}\middle| \begin{matrix} -; a_3 + 1 \\ a_4 + 1, a_5 + 1; - \end{matrix}\right), \quad (11)$$

Substituting (4) into (12) yields

$$F_{P_r^u}(x) = (1-\xi)Pr\left(Q_u \le \sqrt{\frac{x}{k_1}}\right) + \xi Pr\left(Q_u \le \sqrt{\frac{x-k_2}{k_1}}\right) \tag{13}$$

or alternatively

$$F_{P_r^u}(x) = (1-\xi)F_{Q_u}\left(\sqrt{\frac{x}{k_1}}\right) + \xi F_{Q_u}\left(\sqrt{\frac{x-k_2}{k_1}}\right) \tag{14}$$

Hence, the CDF of the instantaneous received power can be given in a closed-form as

$$F_{P_r^u}(x) = (1-\xi)a_1a_2G_{2,3}^{2,1}\left(\frac{\sqrt{\frac{x}{k_1}}}{a_2}\middle| \begin{matrix} 1; a_3+1 \\ a_4+1, a_5+1; 0 \end{matrix}\right) + \xi a_1a_2G_{2,3}^{2,1}\left(\frac{\sqrt{(x-k_2)/k_1}}{a_2}\middle| \begin{matrix} 1; a_3+1 \\ a_4+1, a_5+1; 0 \end{matrix}\right), \tau \ge 0. \tag{15}$$

4) STATISTICAL CHARACTERIZATION OF THE BATTERY RECHARGING TIME

In this study, we introduce novel expressions for the statistical characteristics of the recharge time in RFEH systems. Such expressions can be readily utilized to assess the EH performance over BX channels. According to [38], the instantaneous BRT of node u can be defined as

$$\tau_r^u = \frac{\alpha}{P_r^u} = \frac{D_d C_b V_b}{P_h^u}, \tag{16}$$

where $P_h^u = \eta P_r^u$ is the amount of the harvested power at node u, and α refers to the conversion coefficient, which can be expressed as

$$\alpha = \frac{D_d C_b V_b}{\eta}, \tag{17}$$

where V_b, D_b, C_b, and η denote the constant battery operating voltage, discharge depth, battery capacity, and RF-to-DC signal conversion coefficient, respectively. In this paper, we assume that the battery parameters remain constant over time.

The PDF of battery recharging time can be obtained using (11) through the Jacobian approach using (16). Hence, the PDF of the BRT can be written as follows

$$f_{\tau_r^u}(\tau) = \frac{\alpha}{\tau^2} f_{P_r^u}\left(\frac{\alpha}{\tau}\right) \tag{18}$$

Capitalizing on (11) and (18), the closed-form expression of the PDF of the BRT can be found as

$$f_{\tau_r^u}(\tau) = \frac{\alpha}{\tau^2}\left((1-\xi)\frac{a_1a_2}{2\frac{\alpha}{\tau}}G_{1,2}^{2,0}\left(\frac{\sqrt{\frac{\alpha}{\tau}/k_1}}{a_2}\middle| \begin{matrix} -; a_3+1 \\ a_4+1, a_5+1; - \end{matrix}\right) + \xi\frac{a_1a_2}{2\left(\frac{\alpha}{\tau}-k_2\right)}G_{1,2}^{2,0}\left(\frac{\sqrt{\left(\frac{\alpha}{\tau}-k_2\right)/k_1}}{a_2}\middle| \begin{matrix} -; a_3+1 \\ a_4+1, a_5+1; - \end{matrix}\right), \tau \ge 0, \tag{19}$$

while the CDF of the BRT represents the probability that the BRT is less than or equal to a specified threshold, τ_{th}, i.e., $F_{\tau_r^u}(\tau_{\text{th}}) = P(\tau_r^u \le \tau_{\text{th}})$. By examining (16), it is readily apparent that there is a direct relationship between the CDFs of the received power and the BRT, which can be given as

$$F_{\tau_r^u}(\tau_{\text{th}}) = 1 - F_{P_r^u}\left(\frac{\alpha}{\tau_{\text{th}}}\right) \tag{20}$$

Accordingly, by substituting (15) into (20), we derive a closed-form expression for the CDF of the BRT as

$$F_{\tau_r^u}(\tau) = 1 - (1-\xi)a_1a_2G_{2,3}^{2,1}\left(\frac{\sqrt{\frac{\alpha}{\tau_{th}}/k_1}}{a_2}\middle| \begin{matrix} 1; a_3+1 \\ a_4+1, a_5+1; 0 \end{matrix}\right) - \xi a_1a_2G_{2,3}^{2,1}\left(\frac{\sqrt{\left(\frac{\alpha}{\tau_{th}}-k_2\right)/k_1}}{a_2}\middle| \begin{matrix} 1; a_3+1 \\ a_4+1, a_5+1; 0 \end{matrix}\right), \tau \ge 0. \tag{21}$$

It is worth noting that the nth moment is a key statistical metric that enables the derivation of additional statistics, including the mean value and the variance. The evaluation of the nth moment of the BRT can be obtained by taking the statistical expectation as follows

$$\mu_{\tau_r^u}(n) = \int_0^\infty \tau^n f_{\tau_r^u}(\tau)d\tau \tag{22}$$

Substituting (19) into (22) and by utilizing [39, Eq. (2.24.2.1)] and [39, Eq. (2).24.2.4], the nth moment can be found as in (23) on the bottom of the page. Capitalizing on (23), the mean value and the variance of the BRT can be, respectively, obtained as

$$\bar{\tau}_r^u = \mu_{\tau_r^u}(1), \tag{24}$$

and

$$\sigma_{\tau_r^u}^2 = \mu_{\tau_r^u}(2) - \left(\bar{\tau}_r^u\right)^2, \tag{25}$$

C. NODE-NODE CHANNEL MODEL

For each hop $\hat{h}$ in each route $\hat{w}$, there is a set of channels $\mathcal{C}$ each has a bandwidth of BW. $\mathcal{C}^*_{\hat{w},\hat{h}} \in \mathcal{C}$ represents the set of channels with instantaneous SNR values ($\text{SNR}^{(c)}_{\hat{w},\hat{h}}$, $c \in \mathcal{C}^*$) greater than a particular threshold (γ^*). Also, let $N_u{}^*$, where $N_u{}^* \in N_u$ refers to the nodes that have harvested

$$\mu_{\tau_r^u}(n) = (1-\xi)a_1a_2^{1-2n}\left(\frac{\alpha}{k_1}\right)^n\frac{\Gamma(a_4+1-2n)\Gamma(a_5+1-2n)}{\Gamma(a_3+1-2n)} + \xi\frac{a_1a_2\alpha^n 2^{(a_5+a_4-a_3)}}{\sqrt{\pi}k_2^n\Gamma(n)} \times G_{3,5}^{5,1}\left(\frac{k_2}{4k_1a_2^2}\middle| \begin{matrix} 1; \frac{a_3}{2}+\frac{1}{2}, \frac{a_3}{2}+1 \\ n, \frac{a_4}{2}+\frac{1}{2}, \frac{a_4}{2}+1, \frac{a_5}{2}+\frac{1}{2}, \frac{a_5}{2}+1; - \end{matrix}\right). \tag{23}$$

power greater than a threshold $P_{h_{\text{th}}}$ and accordingly the BRT threshold $\tau_r^* = \frac{D_d C_b V_b}{P_{h_{\text{th}}}}$. In our setup, the Rayleigh distribution is considered to model the links between different nodes. Also, we assume that the transmitted power of node u is equal to the available harvested power. Accordingly, the instantaneous received power over channel $c \in \mathcal{C}^*_{\hat{w},\hat{h}}$ for hop $\hat{h}$ in route $\hat{w}$ can be calculated as follows

$$P^{(c)}_{r_{\hat{h},\hat{w}}} = P^{(c)}_o \left(\frac{d}{d^{(c)}_o}\right)^{-\beta} \left(B^{(c)}_{\hat{h},\hat{w}}\right)^2, \; d \geq d_o, \tag{26}$$

$$P^{(c)}_o = P^u_h G_t G_r \left(\frac{\lambda^{(c)}}{4\pi d^{(c)}_o}\right)^2, \tag{27}$$

where $P^{(c)}_o$, G_t, G_r, $B^{(c)}_{\hat{h},\hat{w}}$, $d^{(c)}_o$ and $\lambda^{(c)}$ represent the pathloss over channel c, the gain of the transmit antenna, the gain of the receive antenna, the channel fading coefficient between any ER pair, reference distance, and the wavelength, respectively. Also, d represents the distance between any two communicating nodes. Utilizing (16) and after some mathematical manipulations, (27) can be rewritten as

$$P^{(c)}_{r_{\hat{h},\hat{w}}} = \frac{\alpha \epsilon^{(c)}_{\hat{h},\hat{w}}}{\tau^u_r}, \tag{28}$$

where $\epsilon^{(c)}_{\hat{h},\hat{w}} = \left(\frac{\lambda^{(c)}\sqrt{G^{(c)}_t G^{(c)}_r} B^{(c)}_{\hat{h},\hat{w}}}{4\pi d^{(c)}_o}\right)^2 \left(\frac{d}{d^{(c)}_o}\right)^{-\beta}$.

Accordingly, the rate achieved by a particular node over the cth channel, hop $\hat{h}$, and route $\hat{p}$ can be calculated as follows

$$R^{(c)}_{\hat{w},\hat{h}} = \rho_u(1-\nu_u) \times \text{BW} \times \log_2\left(1 + \text{SNR}^{(c)}_{\hat{w},\hat{h}}\right), \tag{29}$$

where $\text{SNR}^{(c)}_{\hat{w},\hat{h}} = \frac{P^{(c)}_{r_{\hat{w},\hat{h}}}}{BW \times \mathcal{N}_o}$, therefore (29) can be rewritten as

$$R^{(c)}_{\hat{w},\hat{h}} = \rho_u(1-\nu_u) \times \text{BW} \times \log_2\left(1 + \frac{P^{(c)}_{r_{\hat{w},\hat{h}}}}{BW \times \mathcal{N}_o}\right), \tag{30}$$

where $\mathcal{N}_o$ is the power spectral density (PSD) of the thermal noise. Substituting (28) into (30), the obtainable rate over channel c can be evaluated in terms of the BRT, τ_r, as

$$R^{(c)}_{\hat{w},\hat{h}} = \rho_u(1-\nu_u) \times \text{BW} \times \log_2\left(1 + \frac{\alpha \epsilon^{(c)}_{\hat{h},\hat{w}}}{\tau^u_r \times \text{BW} \times \mathcal{N}_o}\right). \tag{31}$$

According to (31), the calculated rate for each channel in each hop over each path depends on the transmitted power, which is related to the harvested energy at each node. Hence, by optimizing the rate, we implicitly optimize the harvested power, which is inversely related to the BRT.

III. RIS-ASSISTED EAR PROBLEM STATEMENT AND FORMULATION

To enhance the RFEH process, we propose a routing scheme that employs RIS to compensate for the energy losses due to the transmission process.

A. PROBLEM STATEMENT

In order to formulate our problem, we first assume the following: Considering a certain SD pair (U_S and U_D), the whole number of possible routes between the given U_S-U_D pair is $\mathcal{W}$, each route $\hat{w} \in \mathcal{W}$ comprises $\mathcal{H}$ hops. Also, the group of all feasible channels is $\mathcal{C}_{\hat{w},\hat{h}} \in \mathcal{C}, \forall \hat{h} \in \mathcal{H}, \forall \hat{w} \in \mathcal{W}$. The main objective is to determine the best route $\hat{w}^*$ between U_S and U_D, such that the maximum rate is achieved, and accordingly, the BRT is minimized subject to the following constraints:

1) Each device has only one RF transceiver.
2) The received instantaneous SNR at each device must be greater than a certain threshold, γ^*.
3) The BRT at each node does not exceed a specific threshold, τ_r^*.
4) Half-duplex (HD) mode is assumed.

B. THE PROPOSED ROUTE SELECTION AND CHANNEL ALLOCATION ALGORITHM

To study the effect of employing RIS in wireless networks, we propose a routing scheme that consists of three major phases: 1) route discovery, 2) channel allocation, and 3) route selection [40].

1) ROUTE DISCOVERY

To establish a communication between a certain U_S and U_D, the Dynamic Source Routing (DSR) routing protocol is adopted. In this protocol, an on-demand route discovery is only initiated when U_S lacks information on any valid route to the destination in its route cache, which is continuously updated as new routes are learned. Then a Route REQuest (RREQ) message is transmitted from U_S to the whole network. When the first RREQ is received by U_D, U_D dedicates a certain time to acquire a sufficient number of RREQ packets and, hence, identify the feasible routes set $\mathcal{W}$. After that using (30), U_D computes $R^{(c)}_{\hat{w},\hat{h}}$ for the scenario where channel c for hop $\hat{h}$ through each route $\hat{w} \in \mathcal{W}$ is selected. In general, link failures can be handled by maintaining multiple routes to a destination in the nodes' cache. However, this produces an additional control overhead and memory requirements.

2) CHANNEL ALLOCATION

Using the set of the identified routes from the previous stage ($\mathcal{W}$) and the computed $R^{(c)}_{\hat{w},\hat{h}}$, $\forall j, \hat{h}, \hat{w}$, the channel yields the maximum rate (and hence, the minimum BRT) for each hop over each route is selected. Before formulating our problem, we first identify an integer binary variable, namely $\mathcal{Z}^{(c)}_{\hat{w},\hat{h}}$, as follows

$$\mathcal{Z}^{(c)}_{\hat{w},\hat{h}} = \begin{cases} 1, \text{ if channel } c \text{ is assigned to hop } \hat{h} \text{ along route } \hat{w} \\ 0, \text{ otherwise} \end{cases} \tag{32}$$

Given $\mathcal{Z}^{(c)}_{\hat{w},\hat{h}}$, $\hat{w}$, γ^*, τ_r^*, $R^{(c)}_{\hat{w},\hat{h}}$, and $\text{SNR}^{(c)}_{\hat{w},\hat{h}}$, $\forall c \in \mathcal{C}$, $\forall \hat{h} \in \mathcal{H}$, we can formulate the proposed channel allocation problem as follows

$$\max_{\mathcal{Z}^{(c)}_{\hat{w},\hat{h}}} \mathcal{I} = \sum_{\hat{h}=1}^{\mathcal{H}} \sum_{c=1}^{\mathcal{C}} R^{(c)}_{\hat{w},\hat{h}} \mathcal{Z}^{(c)}_{\hat{w},\hat{h}} \tag{33}$$

$$\text{s.t} \quad \sum_{c=1}^{\mathcal{C}} \mathcal{Z}^{(c)}_{\hat{w},\hat{h}} \leq 1, \forall \hat{h} \in \mathcal{H} \tag{33a}$$

$$\text{SNR}^{(c)}_{\hat{w},\hat{h}} \geq \gamma^* \tag{33b}$$

$$\tau_r^u \leq \tau_r^* \tag{33c}$$

In the given optimization problem, Constrain (33a) denotes that each device has only one RF transceiver; hence, one channel can be assigned for each hop. Constrain (33b) denotes that the received instantaneous SNR at each device must be greater than a certain threshold, γ^*. Constrain (33c) denotes that the harvested power at each node should meet the minimum harvested power threshold, $P_{h_{\text{th}}}$. Constraints (33b) and (33c) can be guaranteed by excluding the channels and the nodes that violate these constraints. By examining the optimization problem in (33), it can be noticed that this problem is an NP-hard problem, implying that finding the globally optimal solution in polynomial time is unlikely for large instances. NP-hardness indicates that the problem involves exploring an exponentially growing search space, making it computationally challenging. Assuming a finite number of nodes, available channels, and hops in each path, (33) can be transformed into an Integer Linear Programming (ILP) problem, which can be solved using a branch and bound heuristic algorithm. Assuming that $\Gamma_w^* = [c_1^*, c_2^*, \ldots, c_h^*, \ldots, c_{\mathcal{C}}^*]$ is the optimum solution of the proposed optimization problem, where c_h^* is the optimal channel allocation for hop h in route w. Given Γ_w^*, the rate over each $h \in \mathcal{H}$ along the route w are given by

$$R_{\hat{w},\hat{h}} = R^{(c^*)}_{\hat{w},\hat{h}}, \forall \hat{h} \in \mathcal{H} \tag{34}$$

Given $R_{\hat{w},\hat{h}}$, the rate R of route $\hat{w}$ can be computed as

$$R^{(\hat{w})} = \arg \min R_{\hat{w},\hat{h}}, \ \forall \hat{w} \in \mathcal{W}. \tag{35}$$

3) ROUTE SELECTION

Finally, after choosing the optimal channels, our proposed algorithm picks the route, $\hat{w}^*$, with the maximum rate as

$$R(\hat{w}^*) = \arg \max R^{(\hat{w})}, \ \hat{w} \in \mathcal{W} \tag{36}$$

In the end, the destination U_D notifies the source U_S along $\hat{w}^*$ with their channel allocations and their corresponding rates. A simplified flow-chart is presented in Fig. 3 for the proposed algorithms.

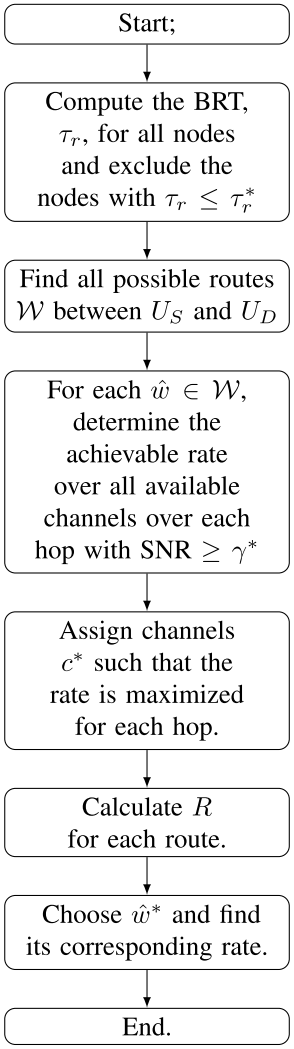

FIGURE 3. Flow-chart of the presented channel allocation and route selection algorithms.

IV. NUMERICAL RESULTS

In this section, we present numerical and simulation results to illustrate the effectiveness of the proposed RIS-assisted routing protocol. We assume that the BS and the RIS are placed within a confined area at coordinates (0.1 m, 0.9 m) and (0 m, 0.8 m), respectively, on a two-dimensional plane. Also, to mimic a larger simulated area, we proportionally scale up these dimensions by a certain factor, where a value of 50 is chosen unless otherwise mentioned. The minimum distance between any two nodes is 5 m, and each node has a coverage range of 15 m. For our analysis, we introduce a cluster of Nu = 30 nodes, distributed randomly within a circular perimeter centered at (0.6 m, 0.5 m) with a radius of 0.4 m. We consider that the nodes operate at the 900 MHz band with four orthogonal channels, each with BW= 5 MHz. As previously mentioned, we adopt Rayleigh and BX fading channel models for the links between node pairs and between the BS and the RIS, respectively. Additionally, we adopt the large-scale fading channel model for the direct links

TABLE 2. The adopted Network Parameters [20], [22].

Parameter	Value
Battery Charging Voltage (V_b)	1.2 V
Battery Capacity (C_b)	10 mAh
Conversion Efficiency (η)	0.5
Discharge Depth (D_d)	0.4
SNR threshold (γ^*)	5 dB
Transmit Antenna Gain(G_t)	0 dBi
Receive Antenna Gain (G_r)	0 dBi
Path loss exponent	2.7

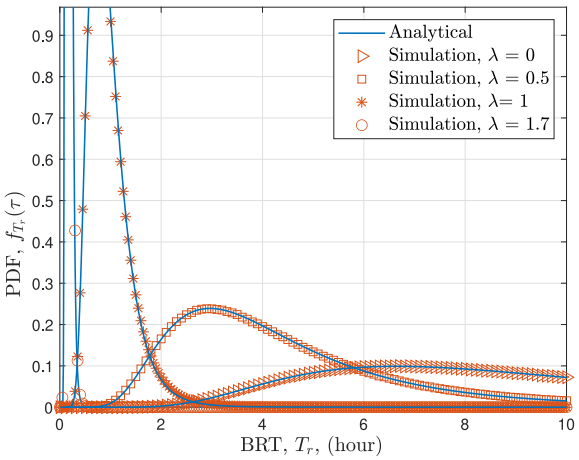

FIGURE 4. The PDF of the BRT of a RIS-assisted WPT system for various values of λ, where $G = 4$, $\Omega = 1$, $m = 1$, $P_s = 10$ dBm, and $\xi = 0$.

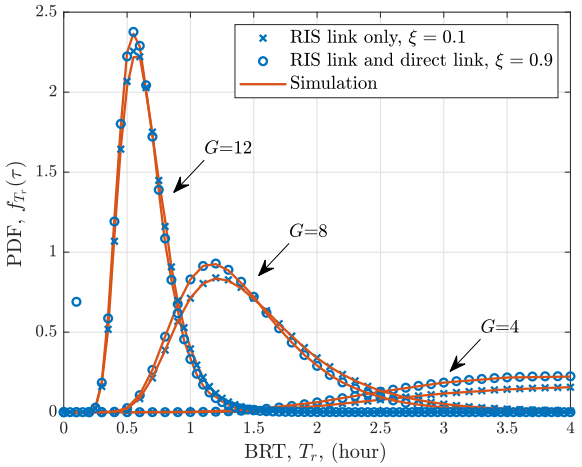

FIGURE 5. The PDF of the BRT of an RIS-assisted WPT system under the presence and absence of a random blockage for various values of G, where λ= 0.7, Ω= 1.5, m= 2, and P_s= 15 dBm.

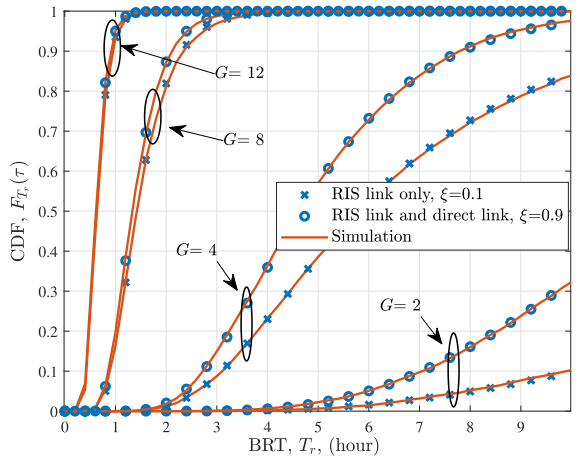

FIGURE 6. The CDF of the BRT of a RIS-assisted WPT system under the presence and absence of a random blockage, for various values of G, where λ = 0.7, Ω = 1.5, m = 2, and P_s = 15 dBm.

under the effect of random blockage. The other parameters are set as follows: noise power of the nodes = -80 dBm, and the minimum harvested power threshold of $P_{h_{\text{th}}} = 10^{-6}$ Watt [41]. For convenience, the remaining parameters are listed in Table 2 [20], [22].

In order to verify the superiority of the proposed algorithm, we compare its performance with the Min hop algorithm as a benchmark model that selects the route with the least hop counts [25]. For the MH algorithm, we adopt our suggested channel assignment mechanism.

Fig. 4 illustrates the analytical and simulated PDF of the E2E BRT over the RIS-assisted single node WPT system under the BX fading channel and with different values of the scale parameter λ. It can be noticed that λ controls the location and the mode height of the BX PDF. It is verified in Fig. 4 the accuracy of the analytical expressions given in (19). Fig. 4 also shows that the BRT of ER nodes decreases as λ increases. More particularly, as λ reduces from 0.5 to 0, the highest possible value of BRT jumps from 3 hours to 7 hours.

Fig. 5, and Fig. 6 depict the analytical and simulated PDF and CDF, respectively, of the E2E RIS-assisted single node WPT system over BX fading channel model. These figures are presented under varying numbers of RIS elements, taking into account scenarios with and without random blockages affecting the direct link. It is observed that shorter battery recharging times can be achieved by increasing the number of RIS elements. Also, the figures show the impact of a random blockage on the PDF of the battery recharging time. It is noted from the figures that the presence of such blockages constrains the efficiency of energy harvesting, consequently leading to a slower battery recharging rate. These analysis offer valuable insights into the interplay among variables like the number of RIS elements, BX channel fading parameters, and the presence of obstructions, all of which collectively shape the energy harvesting process. Understanding these effects aids the proposed routing protocol in making informed choices regarding optimal channel allocation and route selection, thereby facilitating the achievement of elevated data transmission rates. As demonstrated in the figures, the presence of blockage restricts the energy harvesting process, resulting in slower battery recharging. These analysis give insights into how the number of elements, BX parameters, and the presence of a blockage

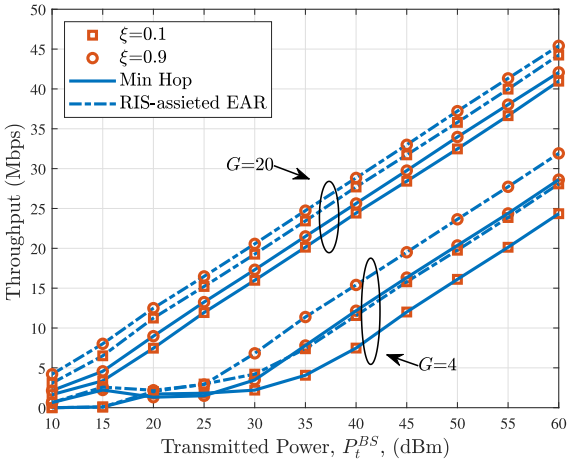

FIGURE 7. E2E throughput vs. transmit power under various number of REs with $\lambda = 0.7$, $\Omega = 1.5$, and $m = 2$.

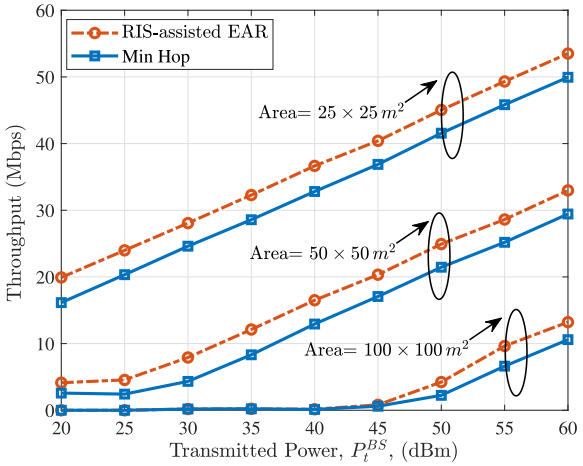

FIGURE 8. E2E throughput vs. transmit power under different scales with $\lambda = 0.7$, $\Omega = 1.5$, $m = 2$, $\xi = 0.9$, and $G = 4$.

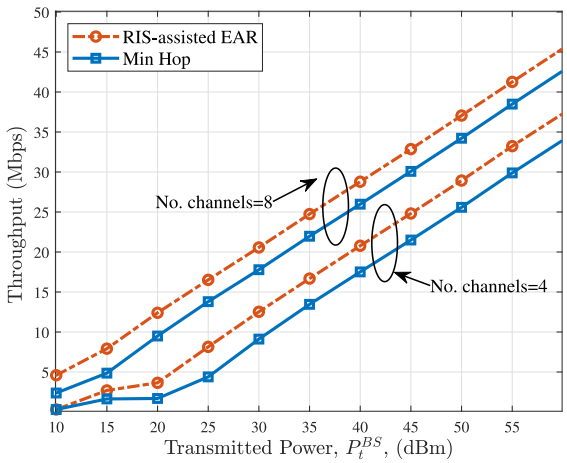

FIGURE 9. E2E network throughput vs. transmit power under various values of channels C with $\lambda = 0.7$, $\Omega = 1.5$, $m = 2$, and $\xi = 0.9$.

can affect the energy harvesting process. The impacts of these factors on the available energy enable the proposed routing protocol to make a well-informed decision regarding channel allocation and path selection to achieve high data transmission rates.

Fig. 7 depicts the E2E network throughput versus the BS transmit power for the proposed RIS-assisted EAR protocol and MH algorithm for $\gamma^* = 5$ dB and different numbers of REs considering the effect of direct link blockage. It is observed that increasing the transmitted power enhances the network throughput. Furthermore, the results show that increasing the number of REs can improve the network performance of both algorithms (i.e., RIS-assisted EAR and MH) for the two scenarios (i.e., $\xi = 0.1$ and $\xi = 0.9$). For instance, at $P_t^{BS} = 40$ dBm, the throughput increases from 15 Mbps to 28 Mbps as G increases from 4 to 20 for our proposed protocol with $\xi = 0.1$. On the other hand, for the MH, the throughput increases from 11 Mbps to 25 Mbps as G increases from 4 to 20 for our proposed protocol with $\xi = 0.1$. This is attributed to the increased number of reflected EM waves, which boosts the amount of energy collected by nodes. Nevertheless, it can be noted that as the number of RIS elements increases, the impact of the direct link diminishes significantly. This implies that the influence of the links established through the RIS gains greater prominence.

Fig. 8 studies the effect of increasing the simulation area on the E2E throughput for the proposed routing protocol. We can note from the figure that the throughput decreases with increasing the simulation area, indicating that WPT systems' efficiency decreases for larger distances or coverage areas. However, it is interesting to note that the proposed protocol works well in small to medium size networks.

The effect of increasing the number of channels provided by the BS is examined in Fig. 9. It is noted that the throughput gets improved as the number of available channels increases due to the high probability of selecting better-quality channels. Also, Fig. 9 shows that our algorithm can achieve a significant throughput when the number of channels increases from 4 to 8 since there is a certain level of freedom to select channels that offer superior quality.

In Fig. 10, we study the impact of using the RIS on the throughput for our proposed EAR protocol. As seen from the figure, the network's overall performance in terms of throughput improves when the RIS is employed. This is due to the ability of RIS to generate additional indirect LoS links, effectively reducing the impact of physical distance. Moreover, the RIS can direct the RF signals from the BS to the RIS and then distribute them to each network node. This enhances the received power and reduces the BRT, consequently enhancing overall network performance.

Finally, Fig. 11 shows the effect of increasing the transmitted power on the number of dead nodes in the two scenarios: 1) with the RIS deployed and 2) without RIS, considering that the direct link between the BS and nodes experiences the BX fading mode. From the figure, we can clearly note that increasing the transmitted power reduces the number of

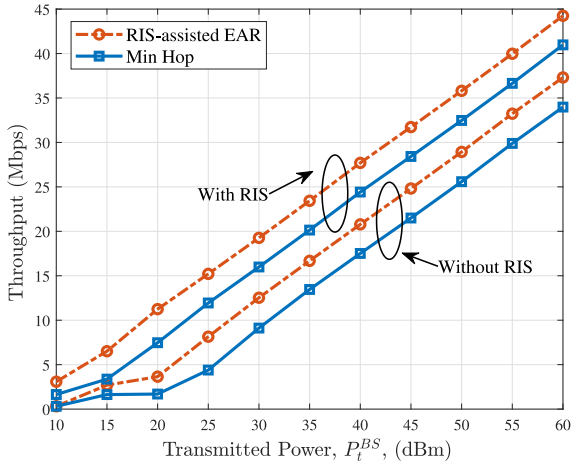

FIGURE 10. The effect of presence of the RIS on the E2E network throughput vs. transmit power, BX fading model.

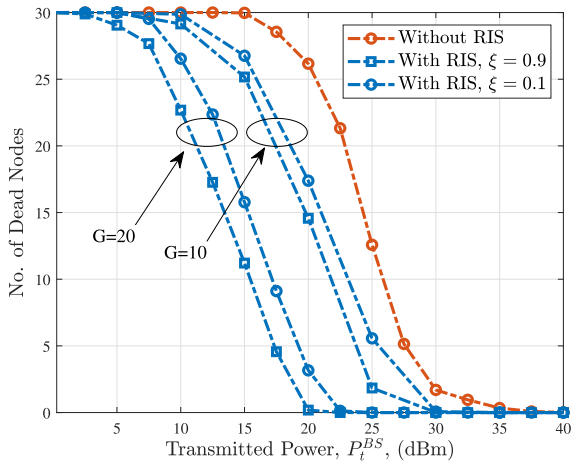

FIGURE 11. The effect of the presence of the RIS on the number of dead nodes vs. transmit power, by considering BX fading model with $\lambda = 0.7$, $\Omega = 1.5$, $m = 2$.

dead nodes in the network for both scenarios. This is because higher transmitted power leads to stronger signals, which can overcome obstacles and attenuation in the environment more effectively. Thus, most of the nodes will receive and harvest sufficient power to enable them to be selected for the transmission phase. Also, the figure illustrates the impact of increasing the number of RIS elements, G, on the number of dead nodes. It is noted that increasing the number of RIS elements significantly reduces the number of dead nodes in the networks. For example, at a transmitted power of 15 dBm and $\xi = 0.1$, the number of the dead nodes is 25 and 15 for $G = 10$ and $G = 20$, respectively. This indicates the significance of RIS in enhancing energy utilization across the network.

In summary, the presented results demonstrated the superiority of our proposed EAR routing algorithm compared to the baseline model (MH algorithm) across different battery capacity levels. Furthermore, the proposed routing protocol showed a significant throughput enhancement compared to the benchmark algorithm. This highlights the importance of the RIS and its applicability to establish indirect LoS links and optimize signal distribution, resulting in improved network performance and substantial throughput gains.

V. CONCLUSION AND FUTURE WORK

We proposed a RIS-assisted energy-aware routing algorithm for multi-hop wireless networks, namely RIS-assisted EAR that considers the BRT of wireless devices in addition to fading channel conditions. The proposed RIS-assisted EAR ensures that the participating nodes have the required harvested energy and, accordingly, the recharging time, thereby improving network throughput. Extensive results have been proposed to compare the performance of RIS-assisted EAR with that of MH and demonstrate the effectiveness of the proposed algorithm to show the superiority of RIS-assisted EAR. Furthermore, we examined the performance of RIS-assisted EAR by comparing its transmit power for various numbers of channels, REs, network size, dead nodes, and the effect of the RIS presence on the network.

To reap the benefits of the RIS, and exploit it at its full potential, we listed below some of our future research and directions.

- Presence of the direct link: Importantly, considering not only deterministic blockage but also fading in the direct link could provide a more realistic assessment of network performance. This would offer a deeper understanding of how RIS technology can be effectively implemented in diverse and dynamic wireless network environments.
- Scalability and network size: Our simulation results showed that the network size inversely affects the throughput, imposing a potential challenge to large networks' scalability. This insight indicates that, despite its good performance in small to medium-sized networks, the performance of the proposed algorithm may decrease in large networks. Moreover, studying the scalability of RIS-assisted routing protocol under different scenarios will provide insights into the protocol's performance and adaptability to different network sizes and conditions.
- Impact of RIS and Energy Harvesting: Our study showed the significant effect of RIS in reducing the BRT and on the network's performance in terms of throughput. Optimization techniques can be applied to optimize the RIS placement to signify the rule of the RIS.
- Leveraging RIS Technology in the Transmission Phase: Another promising area of research is utilizing the RIS during the transmission phase in routing algorithms. This can significantly enhance signal propagation and energy utilization.
- Development of Optimized Scheduling Algorithms: Another crucial thing is to design optimized scheduling algorithms for simultaneous energy recharging through the RIS. Such algorithms can ensure more balanced

energy consumption and harvesting across the network, improving overall network lifetime and performance.

- Addressing the practical challenges: RIS and WPT in IoT networks counter serious challenges such as RIS deploying cost and advanced signal processing techniques for efficient channel estimation. Furthermore, energy efficiency for WPT systems is crucial to ensure reliable communication. This can be achieved by carefully adjusting and optimizing various system parameters, such as device location and power levels.

REFERENCES

[1] R. Gupta, S. Tanwar, S. Tyagi, and N. Kumar, "Tactile Internet and its applications in 5G era: A comprehensive review," *In. J. Commun. Syst.*, vol. 32, no. 14, Sep. 2019, Art. no. e3981.

[2] C. C. González, E. F. Pupo, L. Atzori, and M. Murroni, "Dynamic radio access selection and slice allocation for differentiated traffic management on future mobile networks," *IEEE Trans. Netw. Service Manag.*, vol. 19, no. 3, pp. 1965–1981, Sep. 2022.

[3] R. A. Diab, N. Bastaki, and A. Abdrabou, "A survey on routing protocols for delay and energy-constrained cognitive radio networks," *IEEE Access*, vol. 8, pp. 198779–198800, 2020.

[4] K. W. Choi, L. Ginting, P. A. Rosyady, A. A. Aziz, and D. I. Kim, "Wireless-powered sensor networks: How to realize," *IEEE Trans. Wireless Commun.*, vol. 16, no. 1, pp. 221–234, Jan. 2016.

[5] J. Huang, Y. Zhou, Z. Ning, and H. Gharavi, "Wireless power transfer and energy harvesting: Current status and future prospects," *IEEE Wireless Commun.*, vol. 26, no. 4, pp. 163–169, Aug. 2019.

[6] Z. Zhang, H. Pang, A. Georgiadis, and C. Cecati, "Wireless power transfer—An overview," *IEEE Trans. Ind. Electron.*, vol. 66, no. 2, pp. 1044–1058, May 2019.

[7] C. Liaskos, S. Nie, A. Tsioliaridou, A. Pitsillides, S. Ioannidis, and I. Akyildiz, "A new wireless communication paradigm through software-controlled metasurfaces," *IEEE Commun. Mag.*, vol. 56, no. 9, pp. 162–169, Sep. 2018.

[8] Y. Liu et al., "Reconfigurable intelligent surfaces: Principles and opportunities," *IEEE Commun. Surveys Tuts.*, vol. 23, no. 3, pp. 1546–1577, May 2021.

[9] C. Liaskos, S. Nie, A. Tsioliaridou, A. Pitsillides, S. Ioannidis, and I. Akyildiz, "Realizing wireless communication through software-defined hypersurface environments," in *Proc. IEEE 19th Int. Symp. World Wireless, Mobile Multimedia Netw. (WoWMoM)*, 2018, pp. 14–15.

[10] E. Salahat and N. Yang, "Modeling recharge time of radio frequency energy harvesters in alpha-eta-μ and alpha-kappa-μ fading channels," in *Proc. IEEE Int. Conf. Commun. Workshops (ICC Workshops)*. IEEE, 2018, pp. 1–6.

[11] F. F. Jurado-Lasso, K. Clarke, A. N. Cadavid, and A. Nirmalathas, "Energy-aware routing for software-defined Multihop wireless sensor networks," *IEEE Sensors J.*, vol. 21, no. 8, pp. 10174–10182, Apr. 2021.

[12] K. Haseeb, N. Islam, A. Almogren, I. Ud Din, H. N. Almajed, and N. Guizani, "Secret sharing-based energy-aware and multi-hop routing protocol for IoT based WSNs," *IEEE Access*, vol. 7, pp. 79980–79988, 2019.

[13] Z. Wang, X. Qin, and B. Liu, "An energy-efficient clustering routing algorithm for WSN-assisted IoT," in *Proc. IEEE Wireless Commun. Netw. Conf. (WCNC)*, 2018, pp. 1–6.

[14] Y. Cao, X.-Y. Liu, L. Kong, M.-Y. Wu, and M. K. Khan, "EHR: Routing protocol for energy harvesting wireless sensor networks," in *Proc. IEEE 22nd Int. Conf. Parallel Distrib. Syst. (ICPADS)*, 2016, pp. 56–63.

[15] L. Lin, N. B. Shroff, and R. Srikant, "Asymptotically optimal energy-aware routing for multihop wireless networks with renewable energy sources," *IEEE/ACM Trans. Netw.*, vol. 15, no. 5, pp. 1021–1034, Oct. 2007.

[16] F. Chiti, R. Fantacci, and L. Pierucci, "A green routing protocol with wireless power transfer for Internet of Thing," *J. Sens. Actuator Netw.*, vol. 10, no. 1, pp. 1021–1034, Jan. 2021.

[17] C. Jeong and S. H. Chae, "Simultaneous wireless information and power transfer for multiuser UAV-enabled IoT networks," *IEEE Internet Things J.*, vol. 8, no. 10, pp. 8044–8055, Dec. 2020.

[18] M. Diamanti, P. Charatsaris, E. E. Tsiropoulou, and S. Papavassiliou, "The prospect of reconfigurable intelligent surfaces in integrated access and backhaul networks," *IEEE Trans. Green Commun. Netw.*, vol. 6, no. 2, pp. 859–872, Nov. 2021.

[19] Z. Sadreddini, E. Güler, M. Khalily, and H. Yanikomeroglu, "MRIRS: Mobile ad hoc routing assisted with intelligent reflecting surfaces," *IEEE Trans. Cogn. Commun. Netw.*, vol. 7, no. 4, pp. 1333–1346, May 2021.

[20] D. Altinel and G. K. Kurt, "Statistical models for battery recharging time in RF energy harvesting systems," in *Proc. IEEE Wireless Commun. Netw. Conf. (WCNC)*, 2014, pp. 636–641.

[21] E. Salahat and N. Yang, "Statistical models for battery recharge time from RF energy scavengers in generalized wireless fading channels," in *Proc. IEEE Globecom Workshops (GC Wkshps)*, 2017, pp. 1–6.

[22] L. Mohjazi, S. Muhaidat, Q. H. Abbasi, M. A. Imran, O. A. Dobre, and M. Di Renzo, "Battery recharging time models for reconfigurable intelligent surfaces-assisted wireless power transfer systems," *IEEE Trans. Green Commun. Netw.*, vol. 6, no. 2, pp. 1173–1185, Jun. 2022.

[23] R. Derbas, L. Bariah, S. Muhaidat, P. C. Sofotasios, H. Saleh, and E. Damiani, "Battery recharging time-based routing for power constrained IoT networks," in *Proc. 4th Int. Conf. Adv. Commun. Technol. Netw. (CommNet)*, 2021, pp. 1–5.

[24] H. S. Silva, D. B. T. Almeida, W. J. L. Queiroz, I. E. Fonseca, A. S. R. Oliveira, and F. Madeiro, "Cascaded double Beaulieu-Xie fading channels," *IEEE Commun. Lett.*, vol. 24, no. 10, pp. 2133–2136, Oct. 2020.

[25] C. E. Perkins and P. Bhagwat, "Highly-dynamic destination-sequenced distance-vector routing (DSDV) for mobile computers," in *Proc. SIGCOMM '94 Conf. Commun., Archit., Protocols, Appl.*, 1994, pp. 234–244.

[26] M. Kaur and R. K. Yadav, "Performance analysis of Beaulieu-Xie fading channel with MRC diversity reception," *Trans. Emerg. Telecommun. Technol.*, vol. 31, no. 7, Apr. 2020, Art. no. e3949.

[27] V. Kansal and S. Singh, "Capacity analysis of maximal ratio combining over Beaulieu-Xie fading," *Ann. Telecommun.*, vol. 76, pp. 43–50, Feb. 2021.

[28] J. Hu, Z. Zhang, J. Dang, L. Wu, and G. Zhu, "Performance of decode-and-forward relaying in mixed Beaulieu-Xie and *mathcal*{M} dual-hop transmission systems with digital coherent detection," *IEEE Access*, vol. 7, pp. 138757–138770, 2019.

[29] A. Olutayo, J. Cheng, and J. F. Holzman, "Performance bounds for diversity receptions over a new fading model with arbitrary branch correlation," *EURASIP J. Wireless Commun. Netw.*, vol. 2020, no. 1, pp. 1–26, May 2020.

[30] L. Liu, R. Zhang, and K.-C. Chua, "Wireless information transfer with opportunistic energy harvesting," *IEEE Trans. Wireless Commun.*, vol. 12, no. 1, pp. 288–300, Jan. 2012.

[31] N. C. Beaulieu and X. Jiandong, "A novel fading model for channels with multiple dominant specular components," *IEEE Wireless Commun. Lett.*, vol. 4, no. 1, pp. 54–57, Feb. 2015.

[32] H. Zhang, B. Di, L. Song, and Z. Han, "Reconfigurable intelligent surfaces assisted communications with limited phase shifts: How many phase shifts are enough?" *IEEE Trans. Veh. Technol.*, vol. 69, no. 4, pp. 4498–4502, Apr. 2020.

[33] X. Mu, Y. Liu, L. Guo, J. Lin, and N. Al-Dhahir, "Exploiting intelligent reflecting surfaces in NOMA networks: Joint Beamforming optimization," *IEEE Trans. Wireless Commun.*, vol. 19, no. 10, pp. 6884–6898, Oct. 2020.

[34] M. Abramowitz and I. A. Stegun, *Handbook of Mathematical Functions with Formulas, Graphs, and Mathematical Tables*, vol. 55, U.S. Govt. Print. Office, Washington, DC, USA, 1964.

[35] I. Gradshteyn and I. Ryzhik, *Table of Integrals, Series and Products*, 7th ed. Amsterdam, The Netherlands: Acad. Press, 2007.

[36] F. El Bouanani and D. B. da Costa, "Accurate closed-form approximations for the sum of correlated Weibull random variables," *IEEE Wireless Commun. Lett.*, vol. 7, no. 4, pp. 498–501, Aug. 2018.

[37] L. Bariah, S. Muhaidat, P. C. Sofotasios, F. E. Bouanani, O. A. Dobre, and W. Hamouda, "Large intelligent surface-assisted nonorthogonal multiple access for 6G networks: Performance analysis," *IEEE Internet Things J.*, vol. 8, no. 7, pp. 5129–5140, Apr. 2021.

[38] D. Altinel and G. Karabulut Kurt, "Energy harvesting from multiple RF sources in wireless fading channels," *IEEE Trans. Veh. Technol.*, vol. 65, no. 11, pp. 8854–8864, Nov. 2016.
[39] A. P. Prudnikov et al., *Integrals, and Series: More Special Functions*, vol. 3. New York, NY, USA: Gordon & Breach Sci. Publ., 1990.
[40] H. B. Salameh, S. Otoum, M. Aloqaily, R. Derbas, I. Al Ridhawi, and Y. Jararweh, "Intelligent jamming-aware routing in multi-hop IoT-based opportunistic cognitive radio networks," *Ad Hoc Netw.*, vol. 98, Mar. 2020, Art. no. 102035.
[41] H. Ren, Z. Chen, G. Hu, Z. Peng, C. Pan, and J. Wang, "Transmission design for active RIS-aided simultaneous wireless information and power transfer," *IEEE Wireless Commun. Lett.*, vol. 12, no. 4, pp. 600–604, Apr. 2023.

RAWAN DERBAS received the M.Sc. degree in communication engineering from Yarmouk University, Irbid, Jordan, in 2018. She is currently pursuing the Ph.D. degree in communications engineering with Khalifa University, Abu Dhabi, UAE. Her research interests include reconfigurable intelligent surfaces, spatial modulation techniques, and orthogonal/non-orthogonal multiple access.

SHIMAA NASER (Member, IEEE) is currently a Postdoctoral Fellow with the KU 6G Research Center, Khalifa University. Also, she has teaching experience over 5 years in multiple electrical engineering and computer science courses. She was a Session Chair for local conferences and a member of the Technical Program Committee for multiple IEEE conferences such as IEEE VTC 2022, IEEE ICC 2023, and IEEE 6GNet 2023. Also, she participated in the peer-review process in multiple top IEEE journals such as the IEEE TRANSACTIONS ON COMMUNICATIONS, the IEEE TRANSACTIONS ON WIRELESS COMMUNICATIONS, *Communication Letters*, and *Photonics Journals*. She has authored/co-authored 25+ journal and conference publications and is involved in local and international research collaborations with world-class universities in Canada and U.K. Her research interests include advanced digital signal processing, convex optimization, mobile communication networks, optical wireless communications, ultra-low power networks, MIMO-based communication, and orthogonal/non-orthogonal multiple access.

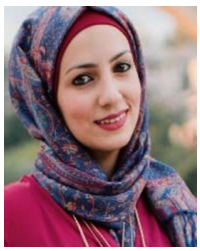

LINA BARIAH (Senior Member, IEEE) received the M.Sc. and Ph.D. degrees in communications engineering from Khalifa University, Abu Dhabi, UAE, in 2015 and 2018, respectively. She was a Visiting Researcher with the Department of Systems and Computer Engineering, Carleton University, Ottawa, ON, Canada, in 2019, and an Affiliate Research Fellow with the James Watt School of Engineering, University of Glasgow, U.K. She is currently a Senior Researcher with the Technology Innovation Institute, an Adjunct Faculty with Khalifa University, and an Adjunct Research Professor with Western University, Canada. He is a Senior Member of IEEE Communications Society, IEEE Vehicular Technology Society, and IEEE WOMEN IN ENGINEERING. She has organized several workshops/special sessions in IEEE flagship conferences including IEEE VTC and IEEE ICC. She was a member of the Technical Program Committee of a number of IEEE conferences, such as ICC and Globecom. She serves as a Session Chair and an Active Reviewer for numerous IEEE conferences and journals. Her research interests include machine learning for wireless communications, large language models, and generative AI for Telecom. She is a Guest Editor of IEEE COMMUNICATION MAGAZINE, IEEE NETWORK MAGAZINE, and IEEE OPEN JOURNAL OF VEHICULAR TECHNOLOGY. She is currently an Associate Editor of IEEE COMMUNICATION LETTERS, an Associate Editor of IEEE OPEN JOURNAL OF THE COMMUNICATIONS SOCIETY, and an Area Editor of *Physical Communication* (Elsevier).

SAMI MUHAIDAT (Senior Member, IEEE) received the Ph.D. degree in electrical and computer engineering from the University of Waterloo, Waterloo, ON, Canada, in 2006. From 2007 to 2008, he was a Postdoctoral Fellow with the Department of Electrical and Computer Engineering, University of Toronto, ON, Canada. From 2008 to 2012, he was an Assistant Professor with the School of Engineering Science, Simon Fraser University, Burnaby, BC, Canada. He is currently a Professor with Khalifa University, Abu Dhabi, UAE. He was also a Visiting Reader with the Faculty of Engineering, University of Surrey, Guildford, U.K. He was a recipient of several scholarships during his undergraduate and graduate studies and the winner of the 2006 Postdoctoral Fellowship Competition. He was a Senior Editor of IEEE COMMUNICATIONS LETTERS, and an Associate Editor of the IEEE TRANSACTIONS ON COMMUNICATIONS, IEEE COMMUNICATIONS LETTERS, and the IEEE TRANSACTIONS ON VEHICULAR TECHNOLOGY. He is currently an Area Editor of the IEEE TRANSACTIONS ON COMMUNICATIONS.

LINA MOHJAZI (Senior Member, IEEE) received the B.Sc. (Hons.) degree in electrical and electronic engineering from United Arab Emirates University, Al Ain, UAE, in 2008, the M.Sc. degree with distinction in electrical and electronic engineering from Khalifa University, Abu Dhabi, UAE, in 2012, and the Ph.D. degree in electrical and electronic engineering from the Institute for Communication Systems, University of Surrey, Guildford, U.K., in 2018. She is currently an Assistant Professor (Lecturer) with the James Watt School of Engineering, University of Glasgow, Glasgow, U.K. Her research interests include beyond 5G wireless technologies, physical-layer optimization and performance analysis, wireless power transfer, machine learning for future wireless systems, and reconfigurable intelligent surfaces. She is an Associate Editor of IEEE COMMUNICATIONS LETTERS and IEEE OPEN JOURNAL OF THE COMMUNICATIONS SOCIETY. She is an Affiliate Member of the Mohammed bin Rashid Academy of Scientists, UAE, and a Fellow of Women's Engineering Society.

OSAMAH S. BADARNEH (Senior Member, IEEE) received the Ph.D. degree in electrical engineering from the École de Technologie Supérieure (ETS), University of Quebec, Canada, in 2009. He joined the German Jordanian University in 2018, where he is currently a Full Professor with the Department of Electrical Engineering. He served as an Adjunct Professor with the Department of Electrical Engineering, ETS, University of Quebec from 2013 to 2018. From 2012 to 2018, he was an Associate Professor with the Department of Electrical Engineering, University of Tabuk. Also, he worked as an Assistant Professor with the Department of Telecommunication Engineering, Yarmouk University, from 2010 to 2012. He is the author of more than 100 publications in scientific journals and international conferences. His research interests focus on wireless communications and networking.

ERNESTO DAMIANI (Senior Member, IEEE) is Full Professor with the Department of Computer Science, Universitàdegli Studi di Milano, where he leads the Secure Service-Oriented Architectures Research Laboratory. He is also the Founding Director of the Center for Cyber-Physical Systems, Khalifa University, UAE. He received the Honorary Doctorate from Institute National des Sciences Appliquees de Lyon, France, in 2017, for his contributions to research and teaching on big data analytics. He has published over 680 peer-reviewed articles and books. His research interests include cybersecurity, big data, and cloud/edge processing. He was a recipient of the 2017 Stephen Yau Award. He serves as an Editor in Chief for the IEEE TRANSACTIONS ON SERVICES COMPUTING. He is a Distinguished Scientist of ACM.